



This is a repository copy of *Ir(III) and Ir(III)/Re(I) complexes of a new bis(pyrazolyl-pyridine) bridging ligand containing a naphthalene-2,7-diyl spacer: Structural and photophysical properties.*

White Rose Research Online URL for this paper:
<http://eprints.whiterose.ac.uk/117596/>

Version: Accepted Version

Article:

Zubaidi, Z.N., Metherell, A.J., Baggaley, E. et al. (1 more author) (2017) Ir(III) and Ir(III)/Re(I) complexes of a new bis(pyrazolyl-pyridine) bridging ligand containing a naphthalene-2,7-diyl spacer: Structural and photophysical properties. *Polyhedron*, 133. pp. 68-74. ISSN 0277-5387

<https://doi.org/10.1016/j.poly.2017.05.017>

Article available under the terms of the CC-BY-NC-ND licence
(<https://creativecommons.org/licenses/by-nc-nd/4.0/>).

Reuse

This article is distributed under the terms of the Creative Commons Attribution-NonCommercial-NoDerivs (CC BY-NC-ND) licence. This licence only allows you to download this work and share it with others as long as you credit the authors, but you can't change the article in any way or use it commercially. More information and the full terms of the licence here: <https://creativecommons.org/licenses/>

Takedown

If you consider content in White Rose Research Online to be in breach of UK law, please notify us by emailing eprints@whiterose.ac.uk including the URL of the record and the reason for the withdrawal request.



eprints@whiterose.ac.uk
<https://eprints.whiterose.ac.uk/>

Ir(III) and Ir(III)/Re(I) complexes of a new bis(pyrazolyl-pyridine) bridging ligand containing a naphthalene-2,7-diyl spacer: structural and photophysical properties

Zainab N. Zubaidi,^{a,b} Alexander J. Metherell,^a Elizabeth Baggaley^a and Michael D. Ward^{a,*}

(a) Department of Chemistry, University of Sheffield, Sheffield S3 7HF, UK

(b) Institute of Technology – Baghdad, Middle Technical University, Iraq.

Abstract

A new bridging ligand has been prepared in which two chelating bidentate pyrazolyl-pyridine termini are connected to a central naphthalene-2,7-diyl core *via* methylene spacer units. This ligand has been used to prepared mononuclear and dinuclear Ir(III) complexes in which $\{\text{Ir}(\text{F}_2\text{ppy})_2\}$ [F_2ppy = cyclometallating anion of 2-(3,5-difluorophenyl)-pyridine] complex fragments are coordinated to one or both of the pyrazolyl-pyridine termini; in addition a heterodinuclear complex has been prepared containing one $\{\text{Ir}(\text{F}_2\text{ppy})_2\}$ unit and one $\{\text{Re}(\text{CO})_3\text{Cl}\}$ unit in the two binding sites. X-ray crystallographic studies show that the bridging naphthyl group lies stacked with a coordinated F_2ppy ligand from a terminal $\{\text{Ir}(\text{F}_2\text{ppy})_2\}$ unit in every case. Luminescence measurements show that the usual strong Ir(III)-centred blue luminescence is substantially quenched by the presence of a low-lying triplet state on the naphthyl group; in the Ir(III)/Re(I) dyad we observe both weak Ir(III)-based emission as well as lower-energy Re(I)-based emission which overlap; Ir(III)→Re(I) energy-transfer occurs on a timescale of < 1 ns as no rise-time for sensitised Re(I)-based emission could be detected, in contrast to other Ir(III)/Re(I) dyads in which the Ir(III)→Re(I) energy-transfer is slower (10 – 100 ns timescale). We ascribe this to the spatial and energetic intermediacy of the naphthyl group whose triplet energy lies between that of the Ir(III) and Re(I) termini, providing an effective conduit for energy-transfer to occur.

Keywords: Iridium(III) complex; Rhenium(I) complex; luminescence; bridging ligand; crystal structures

Introduction

We have extensively investigated the use of bis(pyrazolyl-pyridine) ligands, in which two N,N-chelating termini are connected to an aromatic spacer via flexible methylene groups, for two distinct purposes. Firstly, they have formed the basis of an extensive family of self-assembled coordination cages which display interesting structures and guest binding properties [1]. Secondly, they have been used as a basis for preparing luminescent heterodinuclear complexes in which a blue-luminescent $\{\text{Ir}(\text{ppy})_2(\text{NN})\}^+$ unit [2] is connected to $\{\text{Ln}(\text{hfac})_3(\text{NN})\}$ [3,4] or $\{\text{Re}(\text{CO})_3\text{Cl}(\text{NN})\}$ [5] units in order to investigate phenomena such as inter-component photoinduced energy-transfer and white light emission. The ease with which the basic 3-(2-pyridyl)-1H-pyrazole unit can be functionalised by alkylation at the pyrazolyl N¹ site provides a facile synthetic route into a wide range of such ligands, and has allowed in particular the incorporation of naphthyl units as aromatic spacers between the chelating termini [4,6,7]. This has provided a ‘stepping stone’ for long-distance Ir→Eu photoinduced energy transfer in which the ³naphthyl excited state was demonstrated to be an intermediate between the Ir-based and Eu-based excited states [4]; and the luminescence of the naphthyl unit has also provided added functionality to coordination cages by providing photophysically active units surrounding the central cavity which can interact with bound guests [6,7].

In this paper we report the preparation of a new member of this ligand series, $\text{L}^{27\text{naph}}$, in which the two pyrazolyl-pyridine units are separated by a naphthalene-2,7-diyl spacer: this is a simple isomer of other naphthyl-containing ligands in this series [4,6,7] but, as we have demonstrated, such structural changes can lead to striking differences in coordination behaviour [1a]. In this contribution we report the ligand synthesis and crystal structure, as well as the preparations, structures and photophysical properties of some homonuclear Ir-based complexes and a heterodinuclear Ir/Re complex.

Results and Discussion

(i) Synthesis and structural properties.

The new ligand $\text{L}^{27\text{naph}}$ was prepared by reaction of 3-(2-pyridyl)-1H-pyrazole with 2,7-bis(bromomethyl)naphthalene under basic conditions and purified by chromatography on silica gel; its identity was confirmed by ¹H NMR and mass spectrometric analyses. Recrystallisation from chloroform afforded X-ray quality single crystals; the crystal structure is shown in Fig. 1 (see Table 1 for summary of crystallographic data). Individual bond

distances and angles are unremarkable. The pyridyl and pyrazolyl groups within each potentially chelating unit are mutually transoid. The mean planes of the pyrazolyl-pyridine units are substantially twisted away from the mean plane of the central naphthyl group, with torsion angles about N(41)-C(46) and N(211)-C(26) being 85.3° and 71.5° respectively.

Reaction of $L^{27\text{naph}}$ with the chloride-bridged dimer $[\{\text{Ir}(\text{F}_2\text{ppy})_2(\mu\text{-Cl})\}_2]$ in $\text{CH}_2\text{Cl}_2/\text{MeOH}$ afforded a mixture of mononuclear $[\text{Ir}(\text{F}_2\text{ppy})_2(L^{27\text{naph}})]\text{X}$ and dinuclear $[\{\text{Ir}(\text{F}_2\text{ppy})_2\}_2(\mu\text{-}L^{27\text{naph}})]\text{X}_2$ (where 'X' denotes a nitrate or hexafluorophosphate anion, according to the method used for workup and purification). We abbreviate these hereafter as **Ir•L** and **Ir•L•Ir** respectively. The relative proportions of these products depend on the ratio of components with a higher metal complex:ligand ratio generating more of the dinuclear product. Electrospray mass spectrometry and ^1H NMR spectroscopy were in accord with the formulation of the complexes. Dinuclear **Ir•L•Ir** contains a mixture of two diastereoisomers associated with the chirality of the two metal centres, such that many of the expected ^1H NMR resonances are split into two similar but overlapping components, making the spectrum particularly complex; however the number of signals and their relative intensities is correct. X-ray quality crystals of both products could be obtained from MeCN/ether and their structures are discussed here; coordination sphere bond distances are collected in Table 2.

Fig. 2(a) shows the structure of the complex cation of **Ir•L**. The Ir(III) centre shows the usual 6-coordinate geometry with the two phenylpyridine chelates arranged such that the N atoms are mutually trans and the C atoms are mutually cis [2-5], with the bidentate pyrazolyl-pyridine chelate therefore occupying the two coordination sites trans to the C atoms. The most interesting feature of the structure is that the plane of the pendant naphthyl group is twisted with respect to that of the coordinated pyrazolyl-pyridine unit from which it is pendant, such that it can lie parallel to and overlapping with one of the F_2ppy ligands [containing N(11C) and C(26C)]; atoms in the F_2ppy ligand lie in the range 3.2 – 3.4 Å from the mean plane of the naphthyl group, indicating that they are separated by an ideal π -stacking distance [4]. In addition, the pendant pyrazolyl-pyridine group is oriented such that the pyrazolyl ring [N(41A) – C(45A)] participates in a $\text{CH}\cdots\pi$ interaction with H(14C) from the same F_2ppy ligand, which lies 2.83 Å above the mean plane of the pyrazolyl ring. These π -stacking and $\text{CH}\cdots\pi$ interactions are shown in Fig. 2(b).

Part of the purification of this complex involved chromatography in silica using a MeCN / water / KNO_3 mixture. Although the excess KNO_3 was removed during the final workup, we obtained on occasional a few crystals in the sample of $[\text{Ir}(\text{F}_2\text{ppy})_2(L^{27\text{naph}})](\text{NO}_3)$ which had a different habit; these were analysed crystallographically and turned out to be

$\text{H}[\text{Ir}(\text{F}_2\text{ppy})_2(\text{L}^{27\text{naph}})\text{K}(\text{NO}_3)_3(\text{H}_2\text{O})]$, in which an additional $\{\text{K}(\text{NO}_3)_3(\text{H}_2\text{O})\}^{2-}$ fragment is bound to the pendant pyrazolyl-pyridine site of the $[\text{Ir}(\text{F}_2\text{ppy})_2(\text{L}^{27\text{naph}})]^+$ cation (Fig. 3). We abbreviate this as **Ir•L•K**. In order to accommodate this additional $\{\text{K}(\text{NO}_3)_3(\text{H}_2\text{O})\}^{2-}$ fragment the conformation of the bridging ligand has changed such that the naphthyl group is no longer parallel to and stacked with a F_2ppy ligand around the Ir(III) centre. The coordinated K^+ ion is 9-coordinate, from the N,N-chelating pyrazolyl-pyridine, three bidentate nitrate ligands, and a monodentate water ligand. One of the nitrates and the water ligand exhibit twofold disorder of which only one component is shown in Fig. 3. Most of the K–N and K–O bonds are in the 2.4 – 2.5 Å region, but one of the nitrates [involving N(31S)] is coordinated in a markedly asymmetric manner with the K(1)–O(32S) distance being 2.82 Å. The entire Ir(III) complex unit and its associated bidentate ligand fragments is also disordered over two positions such that every atom occurs in two closely-spaced sites; only the major component is shown in Fig. 3. Given the disorder around both the Ir(1) and K(1) complex units any more detailed analysis of metric parameters is unjustified, but the gross structure of the complex – in particular the substantial changes to the conformation of the bridging ligand which allow it to accommodate a K^+ ion at the secondary binding site – are clear. We note also that the charge on the entire complex is –1, which requires an additional cation somewhere that could not be located, and indeed diffuse electron density that could not be modelled was eliminated from the refinement of this structure using the ‘SQUEEZE’ command in PLATON. Most likely, therefore, the missing charge is a proton in the form of a (possibly disordered) H_3O^+ cation and this is what we have assumed.

Fig 4(a) shows the structure of the dinuclear complex cation of **Ir•L•Ir** which is obtained as a by-product during the preparation of the mononuclear complex **Ir•L** described above. The coordination geometry around each Ir(III) centre is the same as before, but the aromatic stacking between different ligand fragments is more extended, involving both metal termini and the central naphthyl group [Fig. 4(b)]. It is clear that the bridging ligand $\text{L}^{27\text{naph}}$ is partitioned into three approximately mutually perpendicular units: a bidentate pyrazolyl-pyridine chelate coordinating to Ir(1), then the central naphthyl unit, and then the second pyrazolyl-pyridine chelate coordinating to Ir(2). This results in the central naphthyl unit lying sandwiched between one of the cyclometallated F_2ppy units at each Ir(III) centre, forming a three-component π -stacked array in which the mean planes of the F_2ppy units lie ca. 3.4 Å from, and parallel to, the plane of the naphthyl group. As a consequence of this, the central bridging ligand has a helical arrangement (i.e. the successive twists between domains are in

the same sense), and the two metal centres are homochiral: the complex occurs as the $\Delta\Delta/\Lambda\Lambda$ racemic form rather than the Δ/Λ meso form.

Reaction of mononuclear **Ir•L** with $\text{Re}(\text{CO})_5\text{Cl}$ in MeCN afforded the hetero-dinuclear complex $[\{(\text{F}_2\text{ppy})_2\text{Ir}\}(\text{L}^{27\text{naph}})\{\text{Re}(\text{CO})_3\text{Cl}\}](\text{NO}_3)$ (**Ir•L•Re**) in which a $\{\text{Re}(\text{CO})_3\text{Cl}\}$ unit is bound to the second chelating pyrazolyl-pyridine unit of the bridging ligand. Such Ir(III)/Re(I) dyads have been of interest before from the point of view of inter-component energy-transfer between the two metal centres, with slow Ir→Re energy-transfer occurring because of the poor spectroscopic overlap between Ir-based emission and Re-based absorption [5]. The ES mass spectrum conformed formation of the dinuclear complex cation, and incorporation of the $\{\text{Re}(\text{CO})_3\text{Cl}\}$ unit into **Ir•L•Re** is also confirmed by the appearance of a strong IR signal in the ν_{CO} region at 1877 cm^{-1} (with unresolved shoulders). As with dinuclear **Ir•L•Ir**, in **Ir•L•Re** the presence of two chiral metal complex centres results in the complex existing as an approximately 1:1 mixture of diastereoisomers. This means that, in the ^1H NMR spectrum, if a signal from one isomer is sufficiently distinct from the equivalent signal in the other diastereoisomer that it can be separately resolved, signals of apparent intensity 0.5H are observed and this is reflected in the reporting of the NMR data in the experimental section.

The structure of **Ir•L•Re** obtained from crystallographic data is shown in Fig. 5. Again, the bridging ligand is folded such that the pendant naphthyl group lies stacked with a pyridine ring of one of the coordinated F_2ppy ligands at the Ir(III) centre, with separations in the range $3.4 - 3.5\text{ \AA}$ between atoms in the pyridine ring N(11C) – C(16C) and the mean plane of the pendant naphthyl group. The two chelating pyrazolyl-pyridine units lie approximately perpendicular to the central naphthyl group; the Ir•••Re separation is 8.10 \AA . There is twofold disorder between Cl(1) [coordinated to Re(1)] and the CO ligand in the trans position [C(31D) / O(32D)] with only the major component shown in Fig. 5. When Cl(1) is externally directed (as in Fig. 5) there is a water molecule which forms an HOH•••Cl hydrogen-bond with the chloride ligand [O(21S)•••Cl(1) non-bonded distance, 3.21 \AA]. This water molecule is only present when it forms the hydrogen-bond to chloride, which is why it has a site occupancy of 0.64.

(ii) UV/Vis absorption and luminescence properties.

UV/Vis and luminescence spectral data are summarised in Table 3. $\text{L}^{27\text{naph}}$ shows the expected strong absorbances in the UV region. For **Ir•L** and **Ir•L•Ir** we also see in the

UV/Vis spectrum a shoulder at 360 nm which is assigned to formation of the MLCT/LC excited state [2]; this is approximately double the intensity for the dinuclear complex as it is for the mononuclear complex. For **Ir•L•Re** we also expect to see a ¹MLCT absorption associated with the Re(I)/diimine unit [8]; this manifests itself as a weak, lower-energy shoulder at ca. 420 nm compared to mononuclear **Ir•L**.

Luminescence spectra of **Ir•L** and **Ir•L•Ir** show the structured emission with maxima in the blue region that is characteristic of complexes containing the [$\{\text{Ir}(\text{F}_2\text{ppy})_2\}_2(\text{pyridyl-pyrazole})\}^+$ unit and has been assigned as coming from a predominantly ³LC excited state (Fig. 6a) [2,3]. However the luminescence in both cases is weak, with a quantum yield value of <1% in air-equilibrated MeCN: this is over an order of magnitude weaker than we usually see for this type of luminophore [3]. We ascribe this to partial quenching of the Ir(III) unit by energy-transfer to the triplet excited state of the naphthyl group which lies ca. 800 cm⁻¹ below the excited-state energy of the Ir(III) unit [4]. The close association of the pendant naphthyl group with the Ir(III) complex core via the aromatic stacking that is evident in the crystal structures will facilitate this energy-transfer. Time-resolved measurements of both complexes (Table 3) show the presence of at least two emission lifetime components. For **Ir•L** the lifetime values are 36 ns (minor component) and 365 ns (major component). This may be ascribed to the conformational flexibility of the molecule associated with the CH₂ groups in the ligand: in particular the pendant naphthyl group is free to move away from the position seen in the crystal structure where it lies stacked with one of the F₂ppy ligands, and the presence of a range of conformers would result in different rates of internal energy-transfer and hence a decay profile that is not just a single component [9]. For dinuclear **Ir•L•Ir** the time-resolved behaviour is even more complex with at least three emission lifetimes required to obtain a satisfactory fit. The calculated lifetimes of 37, 224 and 767 ns should be treated as approximations: the main point is that a range of conformations of the flexible compound in solution accounts, again, for the multi-exponential emission decay kinetics. We note that the luminescence spectrum of **Ir•L•K** was not significantly changed compared to that of **Ir•L**.

For **Ir•L•Re** the emission spectrum profile is more complex (Fig. 6b), with separate features apparent associated with the weak Ir-based emission (the two sharp, high-energy features between 450 and 500 nm) and also emission from the ³MLCT state of the Re(I) unit (the broader luminescence centred at 525 nm). In this case the weakness of the Re(I)-based emission is normal for this type of chromophore; it is not quenched by the naphthyl group as the naphthyl triplet excited state lies above the ³MLCT level of the Re(I) unit. So we see a combination of substantially quenched Ir(III)-based emission and unquenched, but inherently

weak, Re(I)-based emission that are superimposed on one another. Consistent with this, time-resolved measurements reveal the presence of at least two lifetime components with one short-lived component of ca. 50 ns and a longer-lived component of ca. 400 ns. Importantly, there is no rise-time for the Re-based emission which we saw for a range of other Ir/Re dyads, arising from slow Ir→Re photoinduced energy transfer which causes a grow-in for sensitised Re-based emission [5]. In **Ir•L•Re** the absence of any detectable rise-time for the luminescence means that any sensitisation of Re-based emission happens faster than the lifetime resolution of the instrument (ca. 1 ns). This can be ascribed to the intermediacy of the naphthyl unit which provides a spatial and energetic ‘stepping stone’ for the Ir→Re photoinduced energy transfer process, allowing two fast energy-transfer steps to occur instead of one much slower one [4].

Conclusion

The new ligand reported, $L^{27\text{naph}}$, is an isomer of other ligands from the same family in which the two pyrazolyl-pyridine units are connected to the central naphthyl core at different positions. This changes the geometry of its complexes but does not alter the fact that the naphthyl group quenches the luminescence from the $\{\text{Ir}(\text{F}_2\text{ppy})_2(\text{NN})\}^+$ unit because of its lower-lying triplet state. A consequence of this is that in dinuclear **Ir•L•Re**, Ir→Re photoinduced energy-transfer is fast (< 1 ns) because it can occur in a stepwise manner mediated by the naphthyl unit which acts as a ‘stepping stone’. This contrasts notably with other Ir/Re dyads in which Ir→Re photoinduced energy-transfer is relatively slow (ca. 10 – 100 ns timescale) because of the poor donor/acceptor spectroscopic overlap and the absence of an energetically intermediate ‘stepping stone’.

Experimental section

Materials and instrumentation.

Solvents, metal complex precursors and organic reagents were purchased from Sigma Aldrich or Alfa Aesar. ^1H NMR spectra were recorded on a Bruker Avance-3 400 MHz spectrometer at 298 K using residual solvent signals as internal standards. ESI mass spectra were recorded with a Micromass LCT or Agilent 6530 QTOF-LC/MS instrument. UV-Vis spectra were recorded on a Varian Cary 50 spectrophotometer at room temperature. Luminescence spectra were measured on a Jobin Yvon Fluoromax 4 fluorimeter in air-equilibrated MeCN at room temperature. Luminescence lifetimes were measured using the

time correlated single photon counting (TCSPC) technique with an Edinburgh Instruments “Mini τ ” luminescence lifetime spectrometer, equipped with a 410 nm pulsed diode laser as an excitation source and a Hamamatsu H577303 photomultiplier tube (PMT) detector. The lifetimes were calculated from the measured data using the supplied software.

X-ray crystallography

Data were collected on a Bruker Apex-II diffractometer equipped with a sealed-tube source (Mo-K α radiation). In each case a crystal was removed from the mother liquor, coated with oil, and transferred rapidly to a stream of cold N₂ on the diffractometer to prevent any decomposition due to solvent loss. In all cases, after integration of the raw data, and before merging, an empirical absorption correction was applied (SADABS) based on comparison of multiple symmetry-equivalent measurements [10]. The structures were solved by direct methods and refined by full-matrix least squares on weighted F² values for all reflections using the SHELX suite of programs [11]. For H[Ir(F₂ppy)₂(L^{27naph})K(NO₃)₃(H₂O)] the SQUEEZE function in PLATON [12] was required to remove some residual electron density which could not be modelled and is presumed to arise from disordered solvent molecules; full details are included in the CIF. Pertinent crystallographic data are collected in Table 1, and metal coordination sphere bond distances are collected in Table 2. CCDC 1538622-1538626.

Synthesis of L^{27naph}.

A mixture of 3-(2-pyridyl)pyrazole (0.92 g, 6.36 mmol) and sodium hydride [60% dispersion in mineral oil; 1.58 g, 66.00 mmol] in dry THF (30 cm³) was stirred for 10 minutes under N₂. To this was added a solution of 2,7-bis(bromomethyl)naphthalene (1.00 g, 3.18 mmol) and tetrabutylammonium iodide (20 mg, catalytic) in dry THF (20 cm³). The mixture was heated to 75°C for 24 h. After cooling and filtration, the solvent was removed by rotary evaporation. The residue was purified by column chromatography on silica gel eluting with DCM/MeOH (95:5 v/v) to give L^{27naph} as an off-white solid in 69% yield. ESMS: m/z 443 (M + H)⁺. ¹H NMR (400 MHz, CDCl₃): δ (ppm) 8.46 (1H, d, J 4.8); 7.81 (1H, d, J 7.9); 7.51 (1H, d, J 8.3); 7.42 (1H, td, J 7.8, 1.6); 7.35 (1H, s); 7.24 (1H, d, J 2.2); 7.12 (1H, d, J 8.5); 6.92 (1H, m); 6.82 (1H, d, J 2.2); 5.23 (2H, s). Analysis: found C, 74.6; H, 5.5; N, 18.7%. C₂₈H₂₂N₆•0.5H₂O requires: C, 74.5; H, 5.1; N, 18.6%.

Synthesis of Ir(III) complexes [Ir(F₂ppy)₂(L^{27naph})](NO₃) and [{Ir(F₂ppy)₂]₂(μ -L^{27naph})](PF₆)₂.

A mixture of $L^{27\text{naph}}$ (0.10 g, 2.26 mmol) and $[\{\text{Ir}(\text{F}_2\text{ppy})_2\}(\mu\text{-Cl})_2]$ (0.11 g, 8.81 mmol) was dissolved in degassed DCM/MeOH (3:1, v/v) and then heated to reflux for 18 h under N_2 in the dark. The yellow solution was cooled to room temperature and the solvent removed under reduced pressure. Saturated aqueous KPF_6 solution (20 cm^3) and CH_2Cl_2 (25 cm^3) were added and then the organic layer was extracted, dried over MgSO_4 , filtered and evaporated to dryness to afford the crude product as a yellow oil. This was purified by column chromatography on silica gel eluting with MeCN/aqueous KNO_3 (96:4, v/v).

The first major fraction to elute is mononuclear $[\text{Ir}(\text{F}_2\text{ppy})_2(L^{27\text{naph}})](\text{NO}_3)$ (0.15 g, 63%). ESMS: m/z 1015.24 ($\text{M} - \text{NO}_3$)⁺. ^1H NMR (400 MHz, CD_3CN): δ (ppm) 8.56 (1H, d, J 4.5); 8.34 (1H, d, J 7.9), 8.24 (1H, d, J 8.6), 8.15-8.06 (2H, m), 7.95 (1H, d, J 8.0), 7.89 (1H, t, J 7.8), 7.85-7.79 (2H, m), 7.78-7.67 (3H, m), 7.59 (1H, d, J 8.5), 7.51-7.42 (3H, m), 7.36 (1H, td, J 6.6, 1.3), 7.24 (1H, dd, J 6.4, 4.8), 7.18 (1H, td, J 6.6, 1.2), 6.98 (1H, s), 6.95 (1H, d, J 2.2), 6.92 (2H, d, J 4.0), 6.70 (1H, m), 6.62 (1H, td, J 11.1, 2.3), 6.55-6.41 (2H, m), 5.87 (1H, s), 5.68 (1H, dd, J 8.4, 2.2), 5.51-5.47 (3H, m), 5.30 (1H, dd, J 8.5, 2.2), 5.19 (1H, d, J 17.6). The sample for elemental analysis was analysed as the hexafluorophosphate salt. Analysis: found C, 52.7; H, 3.4; N, 11.2%. $\text{C}_{50}\text{H}_{34}\text{F}_4\text{IrN}_8\text{PF}_6 \cdot 2\text{MeCN}$ requires: C, 52.2; H, 3.3; N, 11.3%.

The second major fraction to elute is dinuclear $[\{\text{Ir}(\text{F}_2\text{ppy})_2\}_2(\mu\text{-}L^{27\text{naph}})](\text{NO}_3)_2$; after removal of solvents and anion metathesis with aqueous KPF_6 this was isolated as $[\{\text{Ir}(\text{F}_2\text{ppy})_2\}_2(\mu\text{-}L^{27\text{naph}})](\text{PF}_6)_2$ in 17% yield. ESMS: m/z 1587.2 ($\text{M} - \text{PF}_6$)⁺. ^1H -NMR (400 MHz, CD_3CN): δ (ppm) 8.35 (1H, t, J 8.9); 8.27-8.19 (2H, m); 8.17-8.06 (1H, m); 7.97-7.86 (1H, m); 7.77-7.65 (2H, m); 7.62-7.48 (1.5H, m); 7.48-7.33 (2.5H, m); 7.30-7.00 (2.5H, m); 6.92 (0.5H, m); 6.87-6.75 (1H, m); 6.70-6.57 (1H, m); 6.54-6.41 (1.5H, m); 6.28 (0.5H, d, J 8.6); 5.88 (0.5H, s); 5.68 (0.5H, m); 5.63-5.50 (1H, m); 5.44 (0.5H, d, J 17.3); 5.35 (0.5H, m); 5.28 (0.5H, m); 5.22-5.10 (1.5H, m). Analysis: found C, 46.4; H, 3.1; N, 8.5%. $\text{C}_{72}\text{H}_{46}\text{F}_8\text{Ir}_2\text{N}_{10}(\text{PF}_6)_2 \cdot 2\text{MeCN}$ requires: C, 46.6; H, 2.7; N, 8.6%.

Synthesis of $[\{\text{F}_2\text{ppy}\}_2\text{Ir}\{L^{27\text{naph}}\}\{\text{Re}(\text{CO})_3\text{Cl}\}](\text{NO}_3)$.

A mixture of $[\text{Ir}(\text{F}_2\text{ppy})_2(L^{27\text{naph}})](\text{NO}_3)$ (22 mg, 0.20 mmol) and $\text{Re}(\text{CO})_5\text{Cl}$ (8 mg, 0.24 mmol) was refluxed in MeCN under N_2 for 24 h. The yellow solution was cooled to room temperature and the solvent removed under reduced pressure. Saturated aqueous KPF_6 solution and DCM were added and then the organic layer was extracted, dried over MgSO_4 , filtered and evaporated to dryness. The crude product was purified on a silica gel column eluting with MeCN:aqueous KNO_3 (98:2, v/v), giving the product as a yellow solid in 26%

yield. ESMS: m/z 1321.2 ($M - PF_6$)⁺. ¹H NMR (400 MHz, CD₃CN): δ (ppm) 8.93 (1H, m); 8.31 (1H, m); 8.25 (1H, m); 8.17-8.13 (2H, m); 8.13-8.04 (3H, m); 7.94-7.83 (2H, m); 7.75-7.66 (2H, m); 7.60 (1H, m); 7.56-7.42 (3.5H, m); 7.41-7.32 (1.5H, m); 7.27-7.20 (1.5H, m); 7.20-7.09 (1.5H, m); 7.09-7.02 (1.5H, m); 6.97 (0.5H, s); 6.81-6.69 (1H, m); 6.65 (1H, ddd, J 2.3, 9.4, 12.5); 6.57-6.47 (1H, m); 6.43 (1H, m); 6.03 (1H, d, J 15.0); 5.93-5.84 (1H, m); 5.82-5.71 (1H, m); 5.71-5.64 (1H, m); 5.50-5.42 (1H, m); 5.34 (1H, dd, 8.6, 2.3); 5.20 (1H, d, J 17.3). The sample for elemental analysis was analysed as the hexafluorophosphate salt. Analysis: found C, 43.3; H, 2.8; N, 7.5%. C₅₃H₃₄ClF₄IrN₈O₃(PF₆)•H₂O requires: C, 42.9; H, 2.4; N, 7.5%.

Appendix A.: Supplementary data. CCDC 1538622–1538626 contain the supplementary crystallographic data for the structures in this paper. These data can be obtained free of charge via <http://www.ccdc.cam.ac.uk/conts/retrieving.html>, or from the Cambridge Crystallographic Data Centre, 12 Union Road, Cambridge CB2 1EZ, UK; fax: [\(+44\) 1223-336-033](tel:+441223336033); or e-mail: deposit@ccdc.cam.ac.uk.

Acknowledgements. We thank the Cultural Attaché of the Embassy of the Republic of Iraq for a PhD studentship (to Z. N. Z.).

Table 1. Crystal parameters, data collection and refinement details for the structures in this paper.

Compound	$L^{27\text{naph}}$	$[\text{Ir}(\text{F}_2\text{ppy})_2(L^{27\text{naph}})](\text{NO}_3) \cdot 2\text{MeCN} \cdot \text{H}_2\text{O}$	$\text{H}[\text{Ir}(\text{F}_2\text{ppy})_2(L^{27\text{naph}})]\text{K}(\text{NO}_3)_3(\text{H}_2\text{O})$
Abbreviation	L	Ir•L	Ir•L•K
Formula	$\text{C}_{28}\text{H}_{22}\text{N}_6$	$\text{C}_{54}\text{H}_{42}\text{F}_4\text{IrN}_{11}\text{O}_4$	$\text{C}_{50}\text{H}_{34}\text{F}_4\text{IrKN}_{11}\text{O}_{10}$
Molecular weight	442.51	1177.18	1256.18
T, K	100(2)	100(2)	1100(2)
Crystal system	Orthorhombic	Monoclinic	Monoclinic
Space group	$P2_12_12_1$	$C2/c$	$I2/a$
a, Å	4.9279(14)	41.4653(17)	17.5169(7)
b, Å	11.578(4)	15.8612(6)	16.6681(7)
c, Å	38.138(12)	15.7425(6)	40.477(2)
α , deg	90	90	90
β , deg	90	1100.806(2)	99.688(4)
γ , deg	90	90	90
V, Å ³	2176.0(12)	10170.1(7)	11649.7(9)
Z	4	8	8
ρ , g cm ⁻³	1.351	1.538	1.432
Crystal size, mm ³	0.25 x 0.16 x 0.11	0.25 x 0.24 x 0.21	0.26 x 0.24 x 0.16
μ , mm ⁻¹	0.083	2.698	2.437
Data, restraints, parameters	2763 / 0 / 309	8977 / 84 / 690	10343 / 1876 / 909
Final R1, wR2 ^a	0.079, 0.167	0.065, 0.183	0.082, 0.215

Compound	$[\{\text{Ir}(\text{F}_2\text{ppy})_2\}_2(\mu-L^{27\text{naph}})](\text{PF}_6)_2 \cdot 6\text{MeCN}$	$[\{\text{F}_2\text{ppy})_2\text{Ir}\}(L^{27\text{naph}})\{\text{Re}(\text{CO})_3\text{Cl}\}](\text{NO}_3) \cdot \text{MeCN} \cdot 0.64\text{H}_2\text{O}$
Abbreviation	Ir•L•Ir	Ir•L•Re
Formula	$\text{C}_{84}\text{H}_{64}\text{F}_{20}\text{Ir}_2\text{N}_{16}\text{P}_2$	$\text{C}_{55}\text{H}_{38.28}\text{ClF}_4\text{IrN}_{10}\text{O}_{6.64}\text{Re}$
Molecular weight	2123.85	1435.32
T, K	110(2)	110(2)
Crystal system	Triclinic	Triclinic
Space group	$P-1$	$P-1$
a, Å	13.6101(9)	12.0080(4)
b, Å	17.2667(11)	15.1430(5)
c, Å	18.3547(13)	15.9523(5)
α , deg	103.115(3)	64.392(2)
β , deg	91.695(3)	77.127(2)
γ , deg	99.224(3)	89.872(2)
V, Å ³	4136.8(5)	2535.41(15)
Z	2	2
ρ , g cm ⁻³	1.705	1.880
Crystal size, mm ³	0.41 x 0.39 x 0.38	0.42 x 0.26 x 0.19
μ , mm ⁻¹	3.354	5.139
Data, restraints, parameters	18878 / 67 / 1101	11413 / 38 / 741
Final R1, wR2 ^a	0.038, 0.123	0.0372, 0.121

^a The value of R1 is based on ‘observed’ data with $I > 2\sigma(I)$; the value of wR2 is based on all data.

Table 2. Summary of coordination-sphere bond distances around the metal complex centres in the crystal structures.

Ir•L

Ir(1)-C(26B)	2.013(8)	Ir(1)-N(11C)	2.047(7)
Ir(1)-C(26C)	2.035(8)	Ir(1)-N(22A)	2.142(7)
Ir(1)-N(11B)	2.044(7)	Ir(1)-N(11A)	2.165(7)

Ir•L•K

Ir(1)-N(11B) ^a	2.011(8)	Ir(2)-N(11Z) ^b	1.97(2)
Ir(1)-C(26C)	2.015(8)	Ir(2)-N(11X)	2.005(18)
Ir(1)-C(26B)	2.033(9)	Ir(2)-C(26Z)	2.03(3)
Ir(1)-N(11C)	2.045(7)	Ir(2)-C(26X)	2.07(2)
Ir(1)-N(22A)	2.083(9)	Ir(2)-N(11Y)	2.115(16)
Ir(1)-N(11A)	2.157(6)	Ir(2)-N(22Y)	2.24(2)

K(1)-O(51S)	2.37(2)	K(1)-N(31A)	2.491(7)
K(1)-O(31S)	2.405(15)	K(1)-N(42A)	2.575(5)
K(1)-O(13S)	2.464(9)	K(1)-O(42S)	2.74(4)
K(1)-O(23S)	2.470(11)	K(1)-N(41S)	2.76(4)
K(1)-O(12S)	2.472(9)	K(1)-O(32S)	2.817(19)
K(1)-O(22S)	2.483(11)		

a Major disorder component associated with Ir(1), see main text

b Minor disorder component associated with Ir(2), see main text

Ir•L•Ir

Ir(1)-C(26B)	1.994(5)	Ir(2)-C(26D)	2.001(5)
Ir(1)-C(26C)	2.021(5)	Ir(2)-C(26E)	2.020(5)
Ir(1)-N(11B)	2.044(4)	Ir(2)-N(11D)	2.043(4)
Ir(1)-N(11C)	2.045(4)	Ir(2)-N(11E)	2.045(4)
Ir(1)-N(42A)	2.145(4)	Ir(2)-N(22A)	2.154(5)
Ir(1)-N(31A)	2.164(4)	Ir(2)-N(11A)	2.159(4)

/continued...

Ir•L•Re

Re(1)-C(21D)	1.929(7)	Ir(1)-C(26C)	2.008(6)
Re(1)-C(11D)	1.935(6)	Ir(1)-C(26B)	2.023(6)
Re(1)-C(31D)	1.967(17)	Ir(1)-N(11C)	2.039(5)
Re(1)-C(41D) ^a	2.01(4)	Ir(1)-N(11B)	2.048(5)
Re(1)-N(42A)	2.188(5)	Ir(1)-N(22A)	2.154(5)
Re(1)-N(31A)	2.201(5)	Ir(1)-N(11A)	2.171(5)
Re(1)-Cl(1)	2.446(4)		
Re(1)-Cl(2) ^b	2.451(8)		

a Major disorder component, see main text

b Minor disorder component, see main text

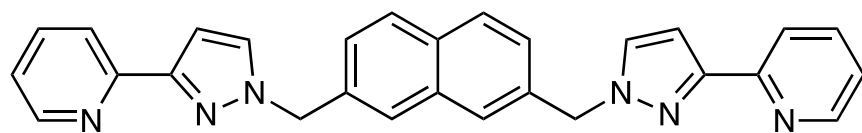
Table 3. Summary of UV/Vis spectroscopic and luminescence data for the complexes (air-equilibrated MeCN, RT).

Complex	UV/Vis [λ_{\max} / nm ($10^{-3} \epsilon$ / $M^{-1} \text{ cm}^{-1}$)]	Emission (λ_{\max} / nm)	ϕ_{lum}	Emission τ / ns
Ir•L	226 (88), 246 (64), 279 (43), 315 (15), 360 (5.5)	455, 485	0.004	36, 365
Ir•L•Ir	228 (136), 244 (123), 290 (67), 360 (13)	455, 485	0.009	37, 224, 767
Ir•L•Re	227 (103), 254 (62), 281 (46), 298 (36), 360 (7.8), 418 (0.5)	455, 485, 520	0.005	52, 330

References

- [1] (a) M. D. Ward, *Chem. Commun.* (2009) 4487;
(b) A. J. Metherell, M. D. Ward, *Dalton Trans.* 45 (2016) 16096;
(c) M. D. Ward, C. A. Hunter, N. H. Williams, *Chem. Lett.* 46 (2017) 2.
- [2] (a) L. Flamigni, A. Barbieri, C. Sabatini, B. Ventura, F. Barigelletti, *Top. Curr. Chem.* 281 (2007) 143;
(b) M. Mydlak, C. Bizzarri, D. Hartmann, W. Sarfert, G. Schmid, L. De Cola, *Adv. Funct. Mater.* 28 (2010) 1812;
(c) E. Orselli, G. S. Kottas, A. E. Konradsson, P. Coppo, R. Fröhlich, L. De Cola, A. van Dijken, M. Büchel, H. Börner, *Inorg. Chem.* 46 (2007) 11082;
(d) T. Sajoto, P. I. Djurovich, A. B. Tamayo, J. Oxgaard, W. A. Goddard, M. E. Thompson, *J. Am. Chem. Soc.* 131 (2009) 9813;
(e) L. He, L. Duan, J. Qiao, R. Wang, P. Wei, L. Wang, Y. Qiu, *Adv. Funct. Mater.* 18 (2008) 2123.
- [3] (a) D. Sykes, A. J. Cankut, N. Mohd Ali, A. Stephenson, S. J. P. Spall, S. C. Parker, J. A. Weinstein, M. D. Ward, *Dalton Trans.* 43 (2014) 6414;
(b) D. Sykes, M. D. Ward, *Chem. Commun.* 47 (2011) 2279;
(c) S. Sykes, I. S. Tidmarsh, A. Barbieri, I. V. Sazanovich, J. A. Weinstein, M. D. Ward, *Inorg. Chem.* 50 (2011) 11323.
(d) A. J. Metherell, C. Curty, A. Zaugg, S. T. Saad, G. H. Dennison, M. D. Ward, *J. Mater. Chem. C* 4 (2016) 9664.
- [4] D. Sykes, S. C. Parker, I. V. Sazanovich, A. Stephenson, J. A. Weinstein, M. D. Ward, *Inorg. Chem.* 52 (2013) 10500.
- [5] S. T. Saad, A. J. Metherell, E. Baggaley, M. D. Ward, *Dalton Trans.* 45 (2016) 11568.
- [6] J. R. Piper, L. Cletheroe, C. G. P. Taylor, A. J. Metherell, J. A. Weinstein, I. V. Sazanovich, M. D. Ward, *Chem. Commun.* 53 (2017) 408;
- [7] (a) N. K. Al-Rasbi, C. Sabatini, F. Barigelletti, M. D. Ward, *Dalton Trans.* (2006) 4769;
(b) I. S. Tidmarsh, T. B. Faust, H. Adams, L. P. Harding, L. Russo, W. Clegg, M. D. Ward, *J. Am. Chem. Soc.* 130 (2008) 15167.
- [8] (a) D. J. Stufkens, *Comments Inorg. Chem.* 13 (1992) 359.
(b) A. Kumar, S.-S. Sun, A. J. Lees, *Top. Organomet. Chem.* 29 (2010) 1.
- [9] S. J. A. Pope, C. R. Rice, M. D. Ward, A. F. Morales, G. Accorsi, N. Armaroli, F. Barigelletti, *J. Chem. Soc. Dalton Trans.* (2001) 2228.

- [10] G. M. Sheldrick, SADABS: A program for absorption correction with the Siemens SMART system, University of Göttingen, Germany, 2008.
- [11] G. M. Sheldrick, *Acta Crystallogr. Sect. A* 64 (2008) 112.
- [12] A. Spek, *J. Appl. Crystallogr.* 36 (2003) 7; P. van der Sluis, A. L. Spek, *Acta Crystallogr. Sect. A: Found. Crystallogr.* 46 (1990) 194.



L27naph

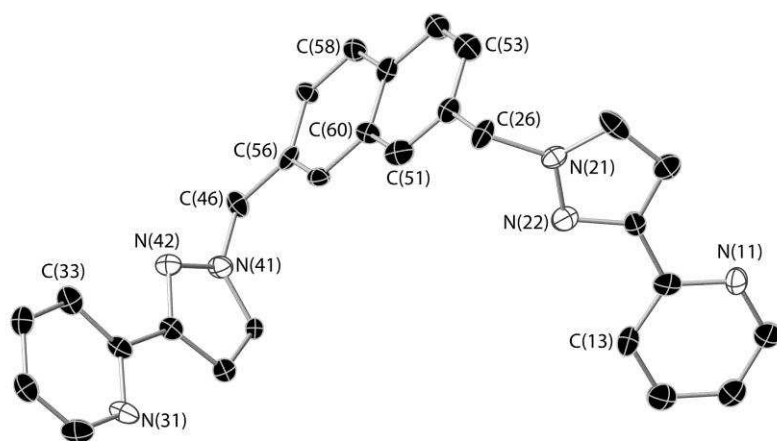


Figure 1 Structure of L^{27naph} from crystallographic data; thermal ellipsoids are at the 40% probability level.

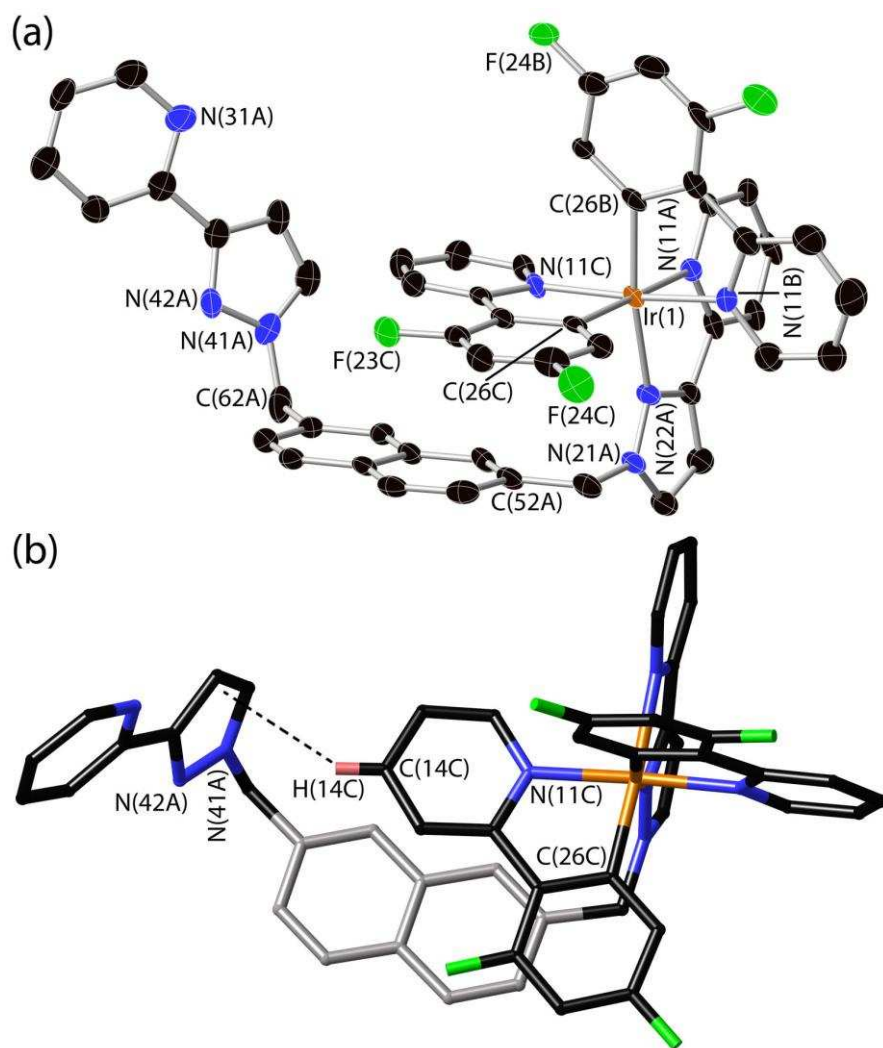


Figure 2 Structure of the complex cation of $[\text{Ir}(\text{F}_2\text{ppy})_2(\text{L}^{27\text{naph}})](\text{NO}_3) \cdot 2\text{MeCN} \cdot \text{H}_2\text{O}$ from crystallographic data. (a) A view showing thermal ellipsoids at the 40% probability level; (b) a view emphasising the aromatic stacking between the naphthyl group (shaded grey) and one of the coordinated F₂ppy ligands, as well as the CH...π interaction of H(14C), shown in pink, and the pendant pyrazolyl ring (see main text).

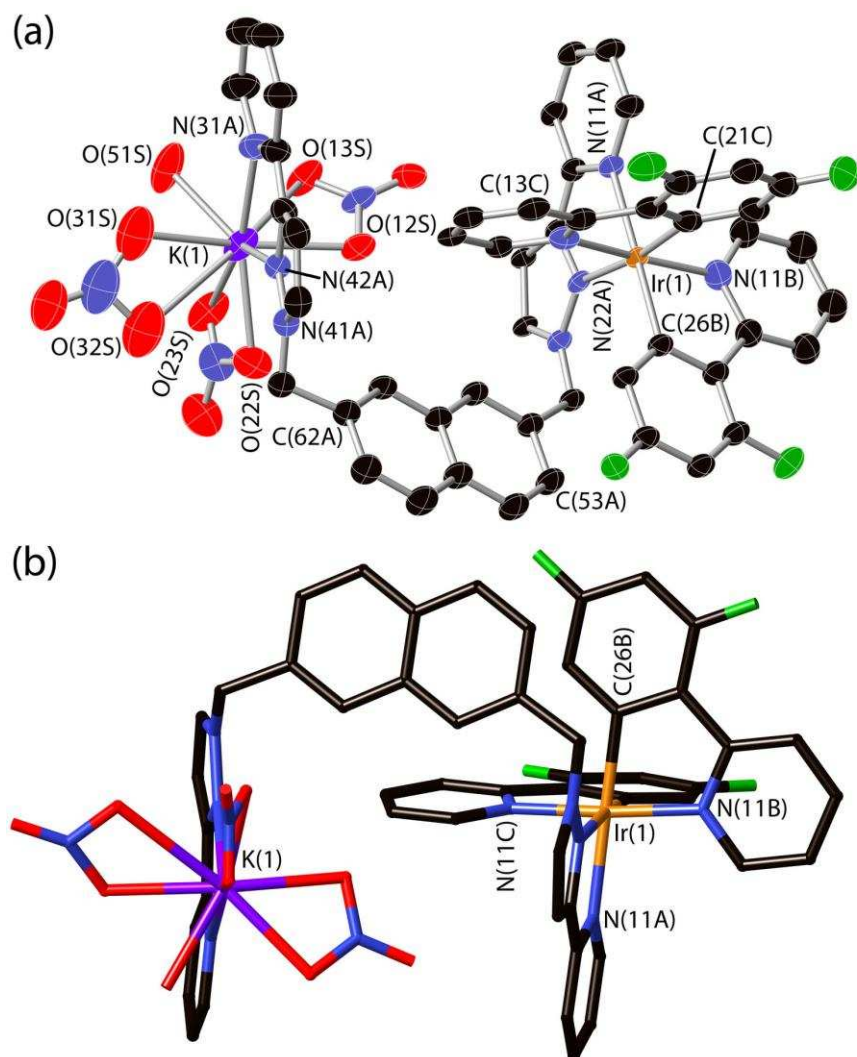


Figure 3 Structure of the complex cation of $\text{H}[\text{Ir}(\text{F}_2\text{ppy})_2(\text{L}^{27\text{naph}})]\text{K}(\text{NO}_3)_3(\text{H}_2\text{O})$ from crystallographic data. (a) A view showing thermal ellipsoids at the 30% probability level; (b) a view emphasising the conformation of the bridging ligand, with the two pyrazolyl-pyridine chelating units being approximately perpendicular to the naphthyl spacer.

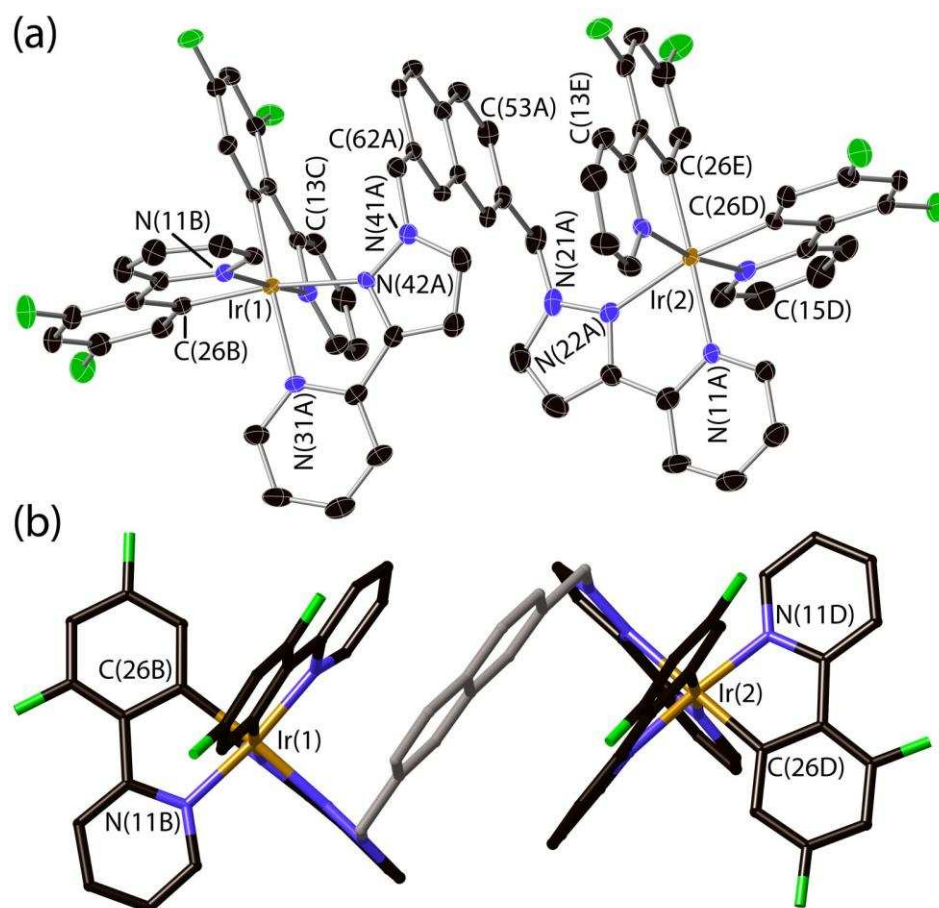


Figure 4 Structure of the complex cation of $[\{\text{Ir}(\text{F}_2\text{ppy})_2\}_2(\mu\text{-L}^{27\text{naph}})](\text{PF}_6)_2 \cdot 6\text{MeCN}$ from crystallographic data. (a) A view showing thermal ellipsoids at the 40% probability level; (b) a view emphasising the helical conformation of the bridging ligand, which results in the central naphthyl group (shaded in grey) sandwiched between two F_2ppy ligands to give a three-component π -stacked array.

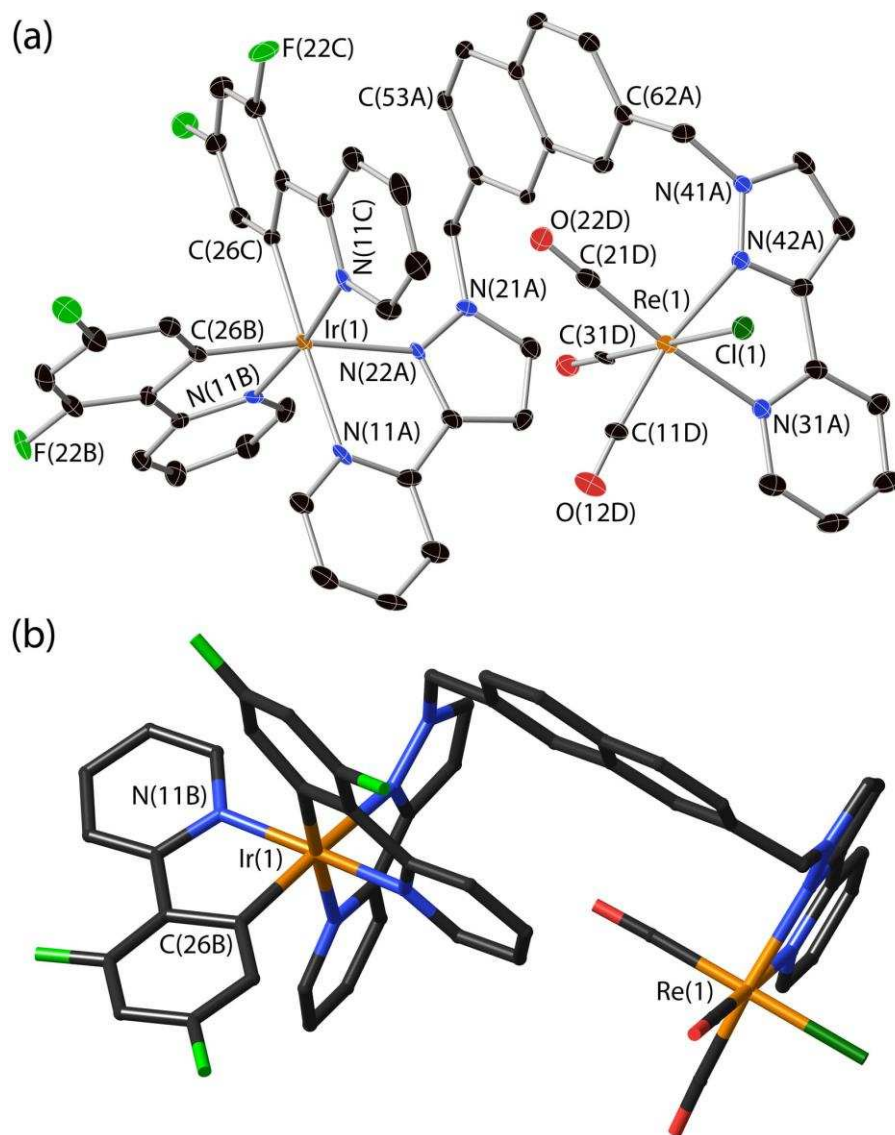


Figure 5 Structure of the complex cation of $[\{(F_2ppy)_2Ir\}(L^{27naph})\{Re(CO)_3Cl\}](NO_3) \cdot MeCN \cdot 0.64H_2O$ from crystallographic data [major disorder component shown involving Cl(1) and C(31D)/O(32D)]. (a) A view showing thermal ellipsoids at the 40% probability level; (b) a view emphasizing a view emphasizing the conformation of the bridging ligand, with the two pyrazolyl-pyridine chelating units being approximately perpendicular to the naphthyl spacer.

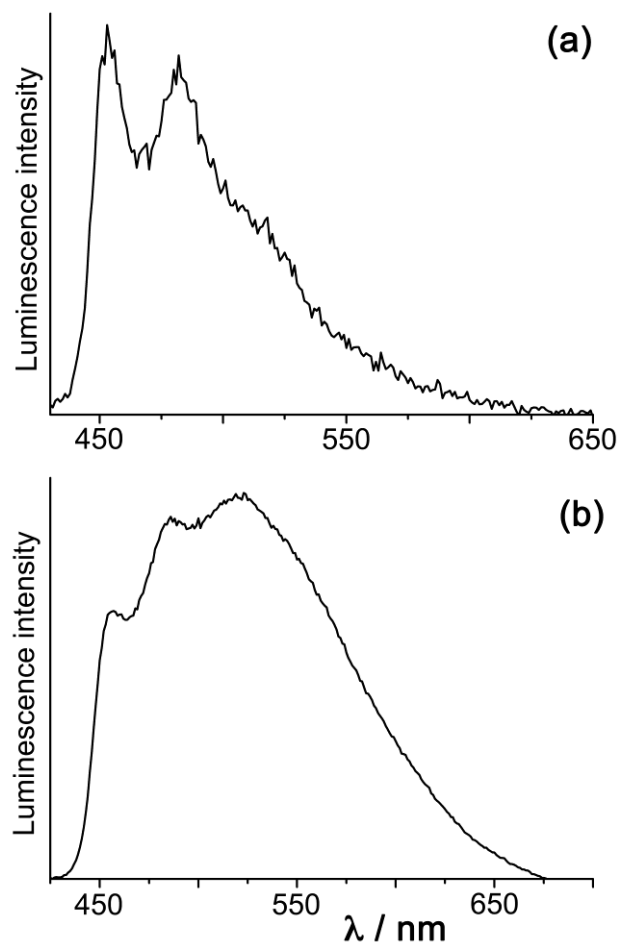


Figure 6 Steady-state emission spectra, in air-equilibrated MeCN at RT, of (a) **Ir•L•Ir** and (b) **Ir•L•Re**.